Cellular and molecular effects of the liposomal mTHPC derivative Foslipos in prostate carcinoma cells in-vitro

Besic Gyenge, E ; Hiestand, S ; Graefe, S ; Walt, H ; Maake, C

Abstract: BACKGROUND: Meso-tetra-hydroxyphenyl-chlorine (mTHPC) is among the most powerful photosensitizers available for photodynamic therapy (PDT). However, the mechanisms leading to cell death are poorly understood. We here focused on changes at DNA and RNA levels after treatment with the liposomal mTHPC derivative Foslipos in vitro. METHODS: After determination of darktoxicity, laser conditions and uptake kinetics, PC-3 prostate carcinoma cells were subjected to PDT with Foslipos, followed by assessment of cell numbers directly (TP0) or 1h (TP1), 2h (TP2), 5h (TP5) and 24h (TP24) after illumination. Nucleic acids had been extracted for evaluation of RNA amounts and integrity as well as for estimation of abasic sites as a measure for DNA damage. Furthermore, expression changes of 84 genes related to oxidative stress were investigated by quantitative polymerase chain reaction. RESULTS: Already at TP0, the number of dead cells was significantly higher after PDT versus controls and at TP24 more than 90% of cells had been destroyed. PDT resulted in a severe damage of both RNA and DNA. Gene expression analyses revealed an impact of PDT on pathways for oxidative and metabolic stress, heat shock, proliferation and carcinogenesis, growth arrest, inflammation, DNA repair and apoptosis signaling. CONCLUSIONS: Mechanisms of Foslipos-mediated PDT comprise a combination of acute and delayed lethal effects in PC-3 cells. The latter may include death processes initiated by nucleic acid damage, activation of stress and growth arrest genes in combination with a reduced capability to adequately cope with oxidative toxicity. Our results will help to better understand molecular photodynamic effects.

DOI: https://doi.org/10.1016/j.pdpdt.2011.02.001

Cellular and molecular effects of the liposomal mTHPC derivative Foslipos in prostate carcinoma cells in-vitro

Emina Besic Gyenge[a+], Seraina Hiestand[a+], Susanna Graefe[b], Heinrich Walt[c], Caroline Maake[a*]

[a]Institute of Anatomy, University of Zurich, Winterthurerstr. 190, 8057 Zurich, Switzerland

[b]biolitec AG, Otto-Schott-Straße 15, 07745 Jena, Germany

[c]Department of Cranio-Maxillo-Facial Surgery, University Hospital Zurich, Frauenklinikstr. 24, 8091 Zurich, Switzerland

+ contributed equally to this work

*Corresponding author,
Institute of Anatomy, University of Zurich,
Winterthurerstr. 190,
8057 Zurich, Switzerland
Tel. +41-44-6355338
Fax. +41-44-6355702
email: cmaake@anatom.uzh.ch

Abstract

Background: Meso-tetra-hydroxyphenyl-chlorine (mTHPC) is among the most powerful photosensitizers available for photodynamic therapy (PDT). However, the mechanisms leading to cell death are poorly understood. We here focuse on changes at DNA and RNA levels after treatment with the liposomal mTHPC derivative Foslipos in-vitro.

Methods: After determination of darktoxicity, laser conditions and uptake kinetics, PC-3 prostate carcinoma cells were subjected to PDT with Foslipos, followed by assessment of cell numbers directly (TP0) or 1h (TP1), 2h (TP2), 5h (TP5) and 24h (TP24) after illumination. Nucleic acids had been extracted for evaluation of RNA amounts and integrity as well as for estimation of abasic sites as a measure for DNA damage. Furthermore, expression changes of 84 genes related to oxidative stress were investigated by quantitative polymerase chain reaction.

Results: Already at TP0, the number of dead cells was significantly higher after PDT versus controls and at TP24 more than 90% of cells had been destroyed. PDT resulted in a severe damage of both RNA and DNA. Gene expression analyses revealed an impact of PDT on pathways for oxidative and metabolic stress, heat shock, proliferation and carcinogenesis, growth arrest, inflammation, DNA repair and apoptosis signaling.

Conclusions: Mechanisms of Foslipos-mediated PDT comprise a combination of acute and delayed lethal effects in PC-3 cells. The latter may include death processes initiated by nucleic acid damage, activation of stress and growth arrest genes in combination with a reduced capability to adequately cope with oxidative toxicity. Our results will help to better understand molecular photodynamic effects.

Introduction

Currently, one of the most powerful second-generation photosensitizers available for photodynamic therapy (PDT) is meso-tetra-hydroxyphenyl-chlorine (mTHPC, Temoporfin), a member of the chlorin family of photosensitizers. The commercial product Foscan gained approval in the EC for palliative PDT treatment of patients with recurrent or refractory head and neck cancers, but it is also under investigation as a promising therapeutic modality for early cancers of the head and neck region, colon adenocarcinoma, non-melanotic skin tumors, pleural mesothelioma, pancreas cancer, hepatoma, carcinoma in-situ of the vulva, malignant brain tumors, ovarian neoplasms, and organ confined prostate cancer [1, 2].

However, Foscan is highly hydrophobic and thus requires the use of organic solvents like alcohols, acetone or ethyl acetate. After intravenous injection in patients, mTHPC molecules tend to aggregate and display very complex biokinetics, such as e.g. a series of subsequent concentration maxima in plasma or limitations in transportation and tumor-uptake [3, 4]. In recent years, these clinically unfavorable characteristics prompted the development of new derivatives of Temoporfin, including the liposomal formulations Foslip and Fospeg (the latter being PEGylated). In addition to the advantage of solvency in hydrophilic media, in first in-vivo and in-vitro studies liposome-incorporated mTHPC had been shown to accumulate faster, selectively and with higher fluorescence in tumor tissues [5-8].

The cell death pathways evoked by oxidative damage in mTHPC-mediated PDT are far from being clear and appear to depend not only on cell type investigated but also on PDT protocol. It had been reported that apoptotic pathways may be initiated [9-12], however, autophagy or necrosis [13] may prevail – especially if high PDT doses are applied [14]. To date only a limited number of studies are available that focus on the spectrum of signaling pathways affected in the course of mTHPC-mediated PDT. Apparently, effects may not only include activation of caspase cascades [10, 11] but also acute-phase response processes [15], and expression changes of heat-shock proteins [16], hypoxia-markers [17], matrix metalloproteinases [18] or cytokines [19]. Since some of these cellular responses may modify, delay or even counteract cell death mechanisms, detailed analyses are highly needed.

With the aim to elucidate pathways leading to and/or interfering with cell death in PDT procedures with liposomal mTHPC we here focus on changes at the DNA and RNA level, as well as on gene expression profiles, using the established prostate carcinoma cell line PC-3 as model system.

Material and Methods

Cell line and reagents

The androgen-independent human prostate carcinoma cell line PC-3 was obtained from the European Collection of Cell Cultures (ECACC). Cells were grown in DMEM+ (1:1 mixture of DMEM and Ham's F-12, without phenol red indicator and pyridoxal HCl, supplemented with 10% fetal calf serum and 1% Penicillin-Streptomycin, 10.000 UI/ml, all purchased from Gibco, Basel, Switzerland) at 37°C and 5% CO_2 in a humid environment. Cells were passaged by trypsinization using 1x trypsin/EDTA (Invitrogen, Basel, Switzerland). As photosensitizer, we used mTHPC encapsulated into dipalmitoylphosphatidylcholine/dipalmitoylphosphatidylglycerol (DPPC/DPPG) liposomes (Foslipos, Biolitec AG, Jena, Germany). Unless otherwise stated, chemicals were purchased from Sigma, Buchs, Switzerland.

Dark toxicity assay

PC-3 cells were plated at a density of 1000 cells per 60 mm Petri dish and allowed to attach for 24 h. Thereafter, Foslipos was added to end concentrations of 0.1, 0.5, 1.0, 5.0, and 10.0 μg/ml, respectively, and incubated for 5h. Then a colony forming assay was performed as described earlier [20]. Briefly, after treatment, cells were washed with PBS and fresh DMEM+ was added. Cells were cultured for another 10 days and colonies were fixed, stained with azur-methylenblue-Giemsa and counted, whereby only colonies containing ≥50 cells were considered. Controls were run under the same conditions, while Foslipos was omitted.

Selection of laser intensity

PC-3 cells were processed as for the dark toxicity assay described above with the exception that cells were exposed to laser light after the 5 h incubation period with Foslipos. Laser intensities of 1, 3, and 5 J/cm^2, respectively, were applied, using a diode laser (Applied Optronics Corporation, USA) at 652 nm and a powermeter (Lightwave

OMM6810B, GMP, Renens, Switzerland). After irradiation, colony forming assays were carried out as described above.

Confocal laser scanning microscopy

PC-3 cells grown on cover slips were incubated with 5 µg/ml Foslipos for 15 min, and 1, 2, 3, 4, and 5 hours, respectively. After a buffer wash, cells were fixed with 4% buffered paraformaldehyde, again washed, coverslipped with Glycergel (Dako, Baar, Switzerland) and analyzed with a confocal laser scanning microscope (SP2, Leica Microsystems, Heerbrugg, Switzerland), using an excitation wavelength of 488nm and detection wavelengths of 580-660nm.

Cell culture treatment

PC-3 cells were plated at a density of $1x10^6$, allowed to recover for 24 h and treated with Foslipos for 5 h at an end concentration of 5 µg/ml. Cells were then exposed to 652 nm laser light reaching a dose of 1 J/cm^2. This experimental setting was termed PDT. Three series of controls were included: (1) omission of the photosensitizer, i.e. replacement of the photosensitizer by buffer, but inclusion of irradiation (IRR), (2) omission of the irradiation and treatment with Foslipos (FOS) and (3) omission of both photosensitizer and irradiation (CO).

After washing all samples with PBS, fresh DMEM+ medium was added and the dishes were placed back in the incubator. Experiments were stopped immediately (i.e. after about 3-4 min) or after 1, 2, 5, and 24 h, respectively, by 2 x 3 min washing and 5 min trypsinization. These five time points are refered to as TP0, TP1, TP2, TP5 and TP24. After centrifugation at 1000 rpm for 5 min, cell pellets were resuspended in 1 ml PBS and either directly used for cell counting or frozen for later nucleic acid analyses.

Cell survival test

Resuspended cells (10 µl) from experimental settings described in "cell culture treatment" were mixed with equal volumes of trypan blue solution (0.5%, Serva, Buchs, Switzerland) and cells (dead and alive) were immediately counted in a Neubauer chamber.

Nucleic acid extractions and quality analyses

From the remainder of resuspended cells (i.e. 990 µl), genomic DNA and total RNA was extracted with the NucleoSpin RNA II kit in conjunction with the NucleoSpin RNA/DNA

buffer set (Macherey-Nagel, Oensingen, Switzerland), following the protocol of the manufacturer. The kit allows for a sequential elution of DNA and RNA from the same cell lysate using a silica membrane filter column and a set of predesigned buffers. Final elution volumes per sample for genomic DNA and total RNA were 100 µl and 60 µl, respectively. Nucleic acid concentrations were determined with a Nanodrop spectrophotometer (ND-1000, Wilmington, DE).

RNA quality was assessed by means of the Agilent 2100 Bioanalyzer equipped with the RNA integrity number (RIN) software algorithm (Agilent, Waldbronn, Germany). For this purpose, total RNA was assayed with the Eukaryote total RNA Nano LabChip kit (Agilent) according to the manufacturer's instructions.

DNA quality was determined with the DNA Damage Quantification kit (MBL, Woburn, MA), that measures the number of apurinic/apyrimidinic sites in DNA lesions. Following the recommendations of the manufacturer, genomic DNA was diluted to 100 µg/ml and labelled with the biotinylated aldehyde reactive probe provided with the kit. Tagged DNA and a tagged standard (provided with the kit) was then bound to a 96-well microplate, followed by an avidin-biotin assay and colorimetric detection at $O.D._{460nm}$. The number of abasic sites within the genomic DNA was determined by comparison with the standard curve.

Gene expression analyses

For gene expression analyses, the PAHS-003 RT^2 Profiler PCR array system was performed according to instructions of the manufacturer (Human stress and toxicity pathways finder array, SuperArray, Frederick, MD). Briefly, 0.5 µg total RNA each from samples TP1 (PDT and CO) and TP5 (PDT and CO) were reverse transcribed with the RT^2 First Strand kit (SuperArray). Resulting cDNA was subjected to quantitative PCR (qPCR) on an ABI 7500 sequence detection system (Applied Biosystems, Rotkreuz, Switzerland) using the supplied 96-well plate format with pre-dispensed specific primer sets and the RT^2 SYBR green/ROX qPCR master mix (SuperArray). Cycling parameters were as follows: 1 cycle for 10min at 95°C and 40 cycles of 15sec at 95°C and 1min at 60°C. Both threshold and baseline values were automatically obtained by the SDS software (Applied Biosystems) and CTs for all wells were exported to the company's data analysis web tool (www. superarray.com).

Statistical analyses

All experiments were carried out in triplicate. Statistical analyses were performed with the StatView software (www.statview.com). All possible pairwise differences between time points as well as between experimental conditions were examined by Fisher's Protected Least Significant Difference (PLSD) tests. P-values less than 0.05 were considered significant.

Results

Experimental conditions

With the aim to establish the appropriate experimental conditions, we first determined the maximal non dark-toxic concentration of Foslipos. We found that colony numbers after treatment with 10 μg/ml Foslipos were significantly lower compared to untreated controls ($p<0.0001$), while all other concentrations of Foslipos used showed no statistically significant effects compared to controls (fig. 1). We thus decided to perform further experiments with 5 μg/ml Foslipos end concentration in the medium. We next investigated the conditions of light exposure with minimal lethal effect at 5 μg/ml Foslipos. 1 J/cm^2 showed the lowest phototoxic effect (data not shown) and was thus choosen for our further study.

Microscopy

Cellular uptake kinetics of Foslipos in PC-3 cells were evaluated on the basis of its intracellular fluorescence (fig. 2). Already after 15 min, a weak signal was detectable within cells. The fluorescence intensity increased steadily over time, reaching a maximum at 4h. It was always diffusely distributed throughout the cytoplasm, with a tendency for a higher signal accumulation in the vicinity of the nucleus. However, the nuclear compartement itself always remained non-fluorescent (fig. 2).

PDT-effects on cell death

As shown in fig. 3, up from the earliest time point investigated (TP0), PDT samples contained statistically significant more dead cells than untreated controls ($p=0.0002$), with a death of about 43% of cells compared to CO. The number of dead cells in PDT samples, however, remained constant up to TP5, while in the TP24-samples this parameter significantly rose ($p<0.0001$) compared to time points before. At TP24, PDT

samples contained only 9% of living cells found in CO. The number of dead cells in IRR and FOS was uniformely low and not statistically different from CO at all time points investigated.

Effects on nucleic acid quantitiy and integrity

Genomic DNA damage was estimated by measuring the amount of apurinic/apyrimidinic sites – a marker for oxidative stress (fig. 4). We found that at all time points measured (TP0, TP1, TP24), the degree of oxidative DNA damage was significantly higher in PDT-treated cells compared to CO samples (TP0, $p<0.0001$; TP1, $p<0.0001$; TP24, $p<0.0001$). DNA quality was also impaired in FOS and IRR samples (compared to CO), however, the difference between PDT and FOS or IRR was still statistically significant at all time points measured (in all cases: $p<0.0001$). Generally, DNA damage of PDT-treated cells was always high, corresponding to an average of 22 abasic sites per 10^5 base pairs at TP0, 18 sites per 10^5 base pairs at TP1 and 16 sites per 10^5 base pairs at TP24.

At all time points investigated, absolute amounts of total RNA in PDT samples were significantly lower than in CO samples. Being stable until (and including) TP2, RNA amounts in PDT samples significantly decreased at TP5, followed by an additional drop at TP24 ($p=0.0009$ and 0.0097, respectively). FOS samples contained RNA amounts comparable to those of CO samples, while IRR samples had a significantly higher RNA content up from TP1 compared to CO. In all control reactions, significant increases in total RNA amounts were found between TP5 and TP24 (IRR: $p<0.0001$; FOS: $p=0.009$; CO: $p=0.0065$). When expressed as a ratio of RNA per (living) cell, RNA content per PDT-treated cell was significantly lower compared to CO from TP0 on ($p=0.0248$), but then remained unchanged over all time points investigated (fig. 5). In CO and FOS the ratio of RNA per cell was comparable and remained constant over time, while IRR samples had significantly more RNA per cell at TP5 compared to CO ($p<0.0001$, fig. 5).

In contrast to all controls, RNA quality was clearly affected by PDT treatment. A small, but statistically significant RNA degradation was already seen at TP0, while RNA integrity was completely maintained under all control conditions (RNA integrity number, RIN, of CO vs. PDT: $p= 0.0022$; IRR vs. PDT: $p=0.001$; FOS vs. PDT: $p=0.001$). In plus, RNA continued to significantly deteriorate over time after PDT, being significantly worse compared to controls at all time points measured (fig. 6).

Effects on gene expression profiles

With the aim to further characterize the effects of Foslipos-mediated PDT, we investigated the expression of 84 genes involved in stress and toxicity pathways by qPCR at TP1 and TP5. Taken together, we found that roughly 57% of all genes investigated changed at least two-fold in expression after PDT. Of these, the majority showed reduced transcript numbers at TP1 (about 83%). Over time, most of the regulated genes (about 54%) maintained their initially changed expression levels. However, at TP5 vs. TP1, about 23% had been further downregulated (HSPA4, CCNC, CCND1, E2F1, NFKB1, ATM, DDB1, BCL2L1, CASP8, CASP10, FASLG), about 12% displayed an further upregulation (CRYAB, DNAJB4, HSPA1A, HSPA1L, HSPA6), and about 10% showed signs of recovery (GSTM3, HSPA2, ERCC3, RAD50, TNFRSF1A, TNFSF10). Tables 1-7 summarize those genes whose expression changed more than twofold between CO vs. PDT and/or over time.

In addition, we found that the following genes are expressed in PC-3 but do not appear to be regulated after PDT: CYP2E1, GPX1, MT2A, PRDX1, DNAJA1, HSF1, HSPA8, HSPB1, HSP90AA2, HSPH1, MIF, GADD45A, GDF15, TP53, CSF2, IL1A, IL6, SERPINE1, CHEK2, ANXA5, and NFKBIA. Genes not expressed in PC-3 cells (neither CO nor PDT) comprise: CRP1A1, CYP7A1, EGR1, EPHX2, FMO1, PTGS1, CCL3, CCL4, CCL21, CXCL10, NOS2A, UGT1A4, CASP1, LTA, and TNF. All gene names are designated according to the HUGO gene name nomenclature (www.genenames.org).

Discussion

Several new strategies are currently under development aiming to improve the efficiency and specificity of PDT. In this context, liposomal photosensitizer preparations are of interest mainly for two reasons: on the one hand they may serve as useful carriers for hydrophobic photoactive molecules in biosystems and on the other hand, they may possess a high payload for targeting molecules. Among others, the photosensitizer mTHPC had been incorporated into different types of liposomes and successfully applied in PDT protocols in-vitro and in-vivo [5, 6, 8, 21-24]. However, the lack of information on molecular effects prompted us to explore cellular mechanisms in PDT with the

DDPG/DDPC liposomal mTHPC derivative Foslipos, using the prostate carcinoma cell line PC-3 as model.

Our microscopic studies on the cellular uptake showed that Foslipos is quickly accumulating in the cytoplasm of PC-3 cells while always sparing the nucleus. We conclude that liposomal preparations do not affect the intracellular distribution since comparable patterns had been reported for mTHPC in a variety of human cell lines [25-27].

As shown before for PC-3-grafted mice [28], PC-3 cells are highly responsive for mTHPC-mediated PDT. Under our experimental conditions we repetitively observed an over 90% reduced cell count 24h after PDT with Foslipos compared to untreated controls. However, the kinetics of this reaction were not linear but rather characterized by a two-step process with an initial death of cells, being already significant a few minutes after light application in PDT (i.e. at TP0) and a second - stronger - boost occuring more than 5h later. Likely, the first “hit” is due to direct detrimental actions of short-lived reactive oxygen species (ROS), that are known to be generated in fractions of seconds after PDT and apparently kill a portion of cells immediately. However, the majority of cells seemed to be merely damaged by ROS and eventually undergo a death process that takes several hours. Whether the latter is related to apoptosis was not within the scope of our experiments and will be the focus of further studies.

To investigate the mechanisms leading to the observed photodynamic effects in more detail we performed experiments to characterize damaging effects on nucleic acids. Results for DNA damage, RNA amount and integrity supports our above observation of an acute PDT effect, that can be documented already shortly after light application.

Since we were unable to localize photosensitizer fluorescence to the cell nucleus, it was surprising that directly after PDT a significant number of DNA strand breaks due to base loss were already detectable. However, results may be explained by mechanisms similar to those observed in a murine glioma cell line, where mTHPC entered the nucleus during light application [29]. The profound and early DNA damage may account for instant cell destruction but – if not repaired - may also result in e.g. blocked DNA replication eventually leading to initiation of death cascades. Notably, even within 24h after PDT no recovery of the number of abasic sites (compared to TP1) was detected, indicating that no

DNA repair had been initiated. At the RNA level these results are complemented by the observation that several important genes associated with DNA repair mechanisms had been transcriptionally downregulated or destroyed after PDT with Foslipos. These include the early DNA damage sensor ATM, DDB1, that is a subunit of the damage-specific DNA binding protein complex, the DNA excision repair endonucleases ERCC1 and ERCC3, the postreplication DNA repair genes RAD23A and RAD50, the uracil-DNA glycosylase UNG and the DNA double strand repair proteins XRCC1 and XRCC2. Furthermore, RNA for PCNA, that is involved in base-excision repair pathways, was reduced. However, low DNA repair capacities have dual effects: they confer a cytotoxicity favorable for PDT by triggering cell death but surviving cells are prone to mutations with unpredictable consequences. In worst case this may result in secondary malignancies after PDT. Our data are in accordance with those in murine gliobastoma cells where mTHPC-PDT also resulted in an immediate DNA damage, however, in this study and others activation of repair mechanisms after PDT had been reported [29-32]. Since our data are in contrast to in-vitro studies in human myeloid leukaemia and nasopharyngeal carcinoma cells where no DNA damage was found after mTHPC-PDT [33, 34], the observed effect may depend on cell line.

The significantly lower readings at TP0 of RNA content per cell after PDT vs. all controls indicate that some RNA was initially destroyed, - presumably by an acute and direct effect of ROS on RNA and not by transcriptional regulation. Not unexpected, the major part of specific genes investigated here thus displayed lower transcript numbers after PDT. Since total RNA consists to 90-95% of ribosomal RNA (rRNA), our data may also point towards an impact of PDT on the translational machinery itself. Interestingly, illumination alone (IRR) lead to a significant increase of RNA amounts measured at TP24, so that actually an interaction of effects elicited by light on the one hand and ROS on the other hand may take place after PDT.

Our further RNA expression studies focusing on established genes involved in stress and toxicity indicated a very complex molecular response of PC-3 cells to mTHPC-mediated PDT, including both higher or lower transcript levels of genes with the potential to either support or counter-act PDT actions. While a higher gene expression is due to an upregulation, lower expression scores may be either a sign of PDT-related RNA

destruction or of true downregulation. The latter may well be a consequence of the observed oxidative DNA damage after PDT. However, with regard to possible damage of rRNA in PDT it is far from clear whether upregulated transcripts are in fact translated into proteins.

Our study reveals reduced levels of genes involved in cellular defense mechanisms against oxidative and metabolic stress. PDT with other photosensitizers are partly in accordance [35, 36] and partly in contrast to our data [37, 38]. Because CAT and SOD1 have been shown to protect cells against phototoxic effects of hematophorphyrin derivative or ALA in vitro [39, 40] and inhibition of SODs results in increased PDT effects [41], we hypothesize that the reduced ability of the cells to cope with oxidative and metabolic stress may constitute an important mechanism for PDT effects with Foslipos. However, as in other studies [42, 43], we found that two antioxidant defense genes (CRYAB and HMOX1) were strongly upregulated. The small heat shock protein CRYAB and the heme oxygenase family member HMOX are known to act as anti-apoptotic molecules that protect cells against oxidative damage [44]. Together with the observation that inhibition of HMOX may increase the efficacy of PDT [43, 45], we propose that – if translated - high levels of HMOX or CRYAB may eventually prevent optimal phototoxic effects.

Expression patterns of heat-shock proteins (HSPs) in our study turned out to be very complex. Several previous papers reported the induction of HSP60, HSP70 or HSP90 after PDT with various photosensitizers [46-51]. However, HSPs consist of large protein families and in our study we found that expression of members may be downregulated or upregulated after PDT with Foslipos. Upregulation of the HSP40 member DNAJB4 as well as HSP70 members HSPA1A, HSPA1L and especially HSPA6, that is only induced by severe stress-stimuli, may mirror the extent of damage in our model but also indicate the presence of a (partly) preserved stress-response system. On the other hand it should be noted that RNA levels of several HSP members investigated here are downregulated. Thus protective mechanisms by HSPs may be rather impaired after PDT with Foslipos. Notably, some of the downregulated HSP70 members belong to essential house keeping genes.

PDT with Foslipos may not only have direct destructive effects on cells but may also block proliferation and induce cell cycle arrest in survivors. Since cell damage is obviously so profound that repair mechanisms are not operative, death pathways are eventually activated. As reported in part previously [52-54], transcripts of cyclin family genes CCNC, CCND1 and CCNG1 as well as of PCNA, a protein crucial for DNA replication, were markedly reduced after PDT in our model thereby possibly leading to a diminished proliferative activity. However, the observed downregulation of cyclin-interacting transcription factor E2F1 may also directly promote cell death, as reported previously for PC-3 cells [55]. The tumor suppressor p53 (TP53) is regarded as a key factor for the regulation of cell growth and death. Interestingly, we and others [56] found that PDT did not change the expression of this gene. However, the expression of one of the main targets of TP53, the cyclin-dependent kinase inhibitor CDKN1A, was reduced after PDT in our study, further supporting an impact of PDT on cell cycle processes. Our data are in contrast to PDT studies that report an increase in CDKN1A [57]. Since MDM2, an important inhibiting factor of p53, was reduced in our study, the ratio of MDM2 to TP53 apparently changed. This may be associated with the potential of increased p53-related pathways and/or reduced p53 degradation followed by cell cycle arrest and apoptosis. Furthermore, we found a strong upregulation of the bZIP transcription factor DDIT3 – notably independent of p53 - after PDT. Since DDIT3 had been implicated in anti-proliferative effects and the induction of apoptosis by certain anti-cancer agents, including in PC-3 cells [58], the observed high levels may have also contributed to growth arrest and apoptotic signaling in our experiment after PDT.

We here report a marked downregulation of IGFBP6 after PDT. Being a relatively specific inhibitor of IGF-II action, high levels of IGFBP-6 had been found to block proliferation and increase apoptosis in-vitro, including in PC-3 cells [59, 60].

In our study, genes involved in apoptosis signaling all displayed reduced transcript numbers. Most of these genes seem to be damaged early – probably due to direct ROS effects. TNFRSF1A, that binds CASP8, as well as both the apoptosis-inducing ligands TNFSF10 and FASLG are almost completely shut down already at TP1 in our model. The biological consequences of fewer apoptosis-promoting BAX in addition to fewer anti-apoptotic BCL2L1 transcripts in PDT with Foslipos are not clear yet. Of interest is

the further reduction of CASP8 and CASP10 RNA over time that is suggestive of a PDT-driven regulatory process. Since many of cell death processes are more adequately investigated at the protein level our data do not generally exclude the activation of apoptotic pathways in Foslipos-mediated PDT. The results may rather be another sign of a breakdown in basic cellular functions.

Taken together, we propose that Foslipos-mediated PDT in PC-3 cells is characterized by a two-stage process. A significant number of cells is disintegrated within minutes, - a process that is likely driven by direct actions of ROS on vital biological components. Even in in-vitro systems that ought to contain a homogeneous population of cells and that uniformly accumulate the photosensitizer, the majority of cells survive this attack. Of course we cannot exclude that this is due to our experimental set-up with e.g. unequal illumination. However, initially surviving cells go into growth arrest and display signs of an oxidative stress response, while many transcripts whose proteins are known to contribute to cellular rescue mechanisms are reduced. Since this is in parallel to severe damages of genomic DNA and the translational system, cells are unable to recover and ultimately die after a delay of several hours.

Acknowledgements

The authors thank Franziska Rossi and Ingrid Briod for their excellent assistance with experiments. The work was supported by the EU FP7 EuroNanoMed ERA-NET grant “TARGET-PDT”.

Legends

Fig. 1

Dark toxicity in PC-3 cells: results of colony forming assays after incubation without or with 0.1-10 mg/ml Foslipos. * p>0.05%

Fig. 2

Uptake of Foslipos into PC-3 cells after (A) 15 min, (B) 1h, (C) 2h, (D) 3h, (E) 4h, and (F) 5h incubation with photosensitizer. Confocal laser scanning microscopy, bar denotes 20 μm.

Fig. 3

Effect of PDT with Foslipos on cell death: direct counts after trypan blue staining directly (TP0) and 1h (TP1), 2h (TP2), 5h (TP5) and 24h (TP24) after light application. CO: no treatment, IRR: with light application, FOS: with incubation of Foslipos.

Fig. 4

Estimation of DNA lesions: binding of an aldehyde reactive probe to DNA after PDT with Foslipos directly (TP0), 1h (TP1) and 24h (TP24) after light application. CO: no treatment, IRR: with light application, FOS: with incubation of Foslipos. Measurements in arbitrary units at $O.D._{460nm}$

Fig. 5

RNA content in µg per 100'000 cells after incubation with Foslipos directly (TP0) and 1h (TP1), 2h (TP2), 5h (TP5) and 24h (TP24) after light application (PDT). CO: no treatment, IRR: with light application, FOS: with incubation of Foslipos.

Fig. 6

(A) Effect of Foslipos-mediated PDT on RNA integrity directly (TP0) and 1h (TP1), 2h (TP2), 5h (TP5) and 24h (TP24) after light application (PDT). CO: no treatment, IRR: with light application, FOS: with incubation of Foslipos. Calculation of the RNA integrity number (RIN), where 10 is intact and 1 is disintegrated. (B) Virtual electrophoresis of total RNA after PDT with Foslipos directly after illumination (TP0) and 24h after light application (TP24). CO: no treatment, IRR: with light application, FOS: with incubation of Foslipos, M: molecular weight marker. Arrow and double arrow denote 28S rRNA and 18S rRNA, respectively.

References

[1] Allison RR, Bagnato VS, Sibata CH. Future of oncologic photodynamic therapy. Future Oncol; 6:929-40.

[2] Brown SB, Brown EA, Walker I. The present and future role of photodynamic therapy in cancer treatment. Lancet Oncol 2004; 5:497-508.

[3] Sasnouski S, Pic E, Dumas D*, et al.* Influence of incubation time and sensitizer localization on meta-tetra(hydroxyphenyl)chlorin (mTHPC)-induced photoinactivation of cells. Radiat Res 2007; 168:209-17.

[4] Triesscheijn M, Ruevekamp M, Out R*, et al.* The pharmacokinetic behavior of the photosensitizer meso-tetra-hydroxyphenyl-chlorin in mice and men. Cancer Chemother Pharmacol 2007; 60:113-22.

[5] Buchholz J, Kaser-Hotz B, Khan T*, et al.* Optimizing photodynamic therapy: in vivo pharmacokinetics of liposomal meta-(tetrahydroxyphenyl)chlorin in feline squamous cell carcinoma. Clin Cancer Res 2005; 11:7538-44.

[6] Svensson J, Johansson A, Grafe S*, et al.* Tumor selectivity at short times following systemic administration of a liposomal temoporfin formulation in a murine tumor model. Photochem Photobiol 2007; 83:1211-9.

[7] Hansch A, Frey O, Gajda M*, et al.* Photodynamic treatment as a novel approach in the therapy of arthritic joints. Lasers Surg Med 2008; 40:265-72.

[8] Lassalle HP, Dumas D, Grafe S, D'Hallewin MA, Guillemin F, Bezdetnaya L. Correlation between in vivo pharmacokinetics, intratumoral distribution and photodynamic efficiency of liposomal mTHPC. J Control Release 2009; 134:118-24.

[9] Kirveliene V, Sadauskaite A, Kadziauskas J, Sasnauskiene S, Juodka B. Correlation of death modes of photosensitized cells with intracellular ATP concentration. FEBS Lett 2003; 553:167-72.

[10] Marchal S, Francois A, Dumas D, Guillemin F, Bezdetnaya L. Relationship between subcellular localisation of Foscan and caspase activation in photosensitised MCF-7 cells. Br J Cancer 2007; 96:944-51.

[11] Bressenot A, Marchal S, Bezdetnaya L, Garrier J, Guillemin F, Plenat F. Assessment of apoptosis by immunohistochemistry to active caspase-3, active caspase-7, or cleaved PARP in monolayer cells and spheroid and subcutaneous xenografts of human carcinoma. J Histochem Cytochem 2009; 57:289-300.

[12] Yow CM, Mak NK, Leung AW, Huang Z. Induction of early apoptosis in human nasopharyngeal carcinoma cells by mTHPC-mediated photocytotoxicity. Photodiagnosis Photodyn Ther 2009; 6:122-7.

[13] Gharehbaghi K, Kubin A, Grusch M*, et al.* Photodynamic action of meta-tetrahydroxyphenylchlorin (mTHPC) on an ovarian cancer cell line. Anticancer Res 2000; 20:2647-52.

[14] Sasnauskiene A, Kadziauskas J, Vezelyte N, Jonusiene V, Kirveliene V. Apoptosis, autophagy and cell cycle arrest following photodamage to mitochondrial interior. Apoptosis 2009.

[15] Merchant S, Sun J, Korbelik M. Dying cells program their expedient disposal: serum amyloid P component upregulation in vivo and in vitro induced by photodynamic therapy of cancer. Photochem Photobiol Sci 2007; 6:1284-9.

[16] Mitra S, Goren EM, Frelinger JG, Foster TH. Activation of heat shock protein 70 promoter with meso-tetrahydroxyphenyl chlorin photodynamic therapy reported by green fluorescent protein in vitro and in vivo. Photochem Photobiol 2003; 78:615-22.

[17] Schouwink H, Oppelaar H, Ruevekamp M*, et al.* Oxygen depletion during and after mTHPC-mediated photodynamic therapy in RIF1 and H-MESO1 tumors. Radiat Res 2003; 159:190-8.

[18] Sharwani A, Jerjes W, Hopper C*, et al.* Photodynamic therapy down-regulates the invasion promoting factors in human oral cancer. Arch Oral Biol 2006; 51:1104-11.

[19] Yom SS, Busch TM, Friedberg JS*, et al.* Elevated serum cytokine levels in mesothelioma patients who have undergone pleurectomy or extrapleural pneumonectomy and adjuvant intraoperative photodynamic therapy. Photochem Photobiol 2003; 78:75-81.

[20] Muller S, Walt H, Dobler-Girdziunaite D, Fiedler D, Haller U. Enhanced photodynamic effects using fractionated laser light. J Photochem Photobiol B 1998; 42:67-70.

[21] Bombelli C, Caracciolo G, Di Profio P*, et al.* Inclusion of a photosensitizer in liposomes formed by DMPC/gemini surfactant: correlation between physicochemical and biological features of the complexes. J Med Chem 2005; 48:4882-91.

[22] Pegaz B, Debefve E, Ballini JP*, et al.* Photothrombic activity of m-THPC-loaded liposomal formulations: pre-clinical assessment on chick chorioallantoic membrane model. Eur J Pharm Sci 2006; 28:134-40.

[23] D'Hallewin MA, Kochetkov D, Viry-Babel Y*, et al.* Photodynamic therapy with intratumoral administration of Lipid-Based mTHPC in a model of breast cancer recurrence. Lasers Surg Med 2008; 40:543-9.

[24] Dragicevic-Curic N, Scheglmann D, Albrecht V, Fahr A. Temoporfin-loaded invasomes: development, characterization and in vitro skin penetration studies. J Control Release 2008; 127:59-69.

[25] Teiten MH, Bezdetnaya L, Merlin JL*, et al.* Effect of meta-tetra(hydroxyphenyl)chlorin (mTHPC)-mediated photodynamic therapy on sensitive and multidrug-resistant human breast cancer cells. J Photochem Photobiol B 2001; 62:146-52.

[26] Leung WN, Sun X, Mak NK, Yow CM. Photodynamic effects of mTHPC on human colon adenocarcinoma cells: photocytotoxicity, subcellular localization and apoptosis. Photochem Photobiol 2002; 75:406-11.

[27] Kiesslich T, Berlanda J, Plaetzer K, Krammer B, Berr F. Comparative characterization of the efficiency and cellular pharmacokinetics of Foscan- and Foslip-based photodynamic treatment in human biliary tract cancer cell lines. Photochem Photobiol Sci 2007; 6:619-27.

[28] Sehgal I, Sibrian-Vazquez M, Vicente MG. Photoinduced cytotoxicity and biodistribution of prostate cancer cell-targeted porphyrins. J Med Chem 2008; 51:6014-20.

[29] Rousset N, Keminon E, Eleouet S*, et al.* Use of alkaline Comet assay to assess DNA repair after m-THPC-PDT. J Photochem Photobiol B 2000; 56:118-31.

[30] Ricci F, Pucci S, Sesti F, Missiroli F, Cerulli L, Spagnoli LG. Modulation of Ku70/80, clusterin/ApoJ isoforms and Bax expression in indocyanine-green-mediated photo-oxidative cell damage. Ophthalmic Res 2007; 39:164-73.

[31] Yang ZZ, Li MX, Zhang YS*, et al.* Knock down of the dual functional protein apurinic /apyrimidinic endonuclease 1 enhances the killing effect of hematoporphrphyrin derivative-mediated photodynamic therapy on non-small cell lung cancer cells in vitro and in a xenograft model. Cancer Sci 2009.

[32] Akramiene D, Aleksandraviciene C, Grazeliene G*, et al.* Potentiating effect of beta-glucans on photodynamic therapy of implanted cancer cells in mice. Tohoku J Exp Med 2010; 220:299-306.

[33] McNair FI, Marples B, West CM, Moore JV. A comet assay of DNA damage and repair in K562 cells after photodynamic therapy using haematoporphyrin derivative, methylene blue and meso-tetrahydroxyphenylchlorin. Br J Cancer 1997; 75:1721-9.

[34] Yow CM, Chen JY, Mak NK, Cheung NH, Leung AW. Cellular uptake, subcellular localization and photodamaging effect of temoporfin (mTHPC) in nasopharyngeal carcinoma cells: comparison with hematoporphyrin derivative. Cancer Lett 2000; 157:123-31.

[35] Du HY, Olivo M, Tan BK, Bay BH. Photoactivation of hypericin down-regulates glutathione S-transferase activity in nasopharyngeal cancer cells. Cancer Lett 2004; 207:175-81.

[36] Luo J, Li L, Zhang Y*, et al.* Inactivation of primary antioxidant enzymes in mouse keratinocytes by photodynamically generated singlet oxygen. Antioxid Redox Signal 2006; 8:1307-14.

[37] El-Missiry MA, Abou-Seif M. Photosensitization induced reactive oxygen species and oxidative damage in human erythrocytes. Cancer Lett 2000; 158:155-63.

[38] Krusekopf S, Roots I. St. John's wort and its constituent hyperforin concordantly regulate expression of genes encoding enzymes involved in basic cellular pathways. Pharmacogenet Genomics 2005; 15:817-29.

[39] Hirakawa K, Mori M, Yoshida M, Oikawa S, Kawanishi S. Photo-irradiated titanium dioxide catalyzes site specific DNA damage via generation of hydrogen peroxide. Free Radic Res 2004; 38:439-47.

[40] Chekulayeva LV, Shevchuk IN, Chekulayev VA, Ilmarinen K. Hydrogen peroxide, superoxide, and hydroxyl radicals are involved in the phototoxic action of hematoporphyrin derivative against tumor cells. J Environ Pathol Toxicol Oncol 2006; 25:51-77.

[41] Golab J, Nowis D, Skrzycki M*, et al.* Antitumor effects of photodynamic therapy are potentiated by 2-methoxyestradiol. A superoxide dismutase inhibitor. J Biol Chem 2003; 278:407-14.

[42] Nowis D, Legat M, Grzela T*, et al.* Heme oxygenase-1 protects tumor cells against photodynamic therapy-mediated cytotoxicity. Oncogene 2006; 25:3365-74.

[43] Frank J, Lornejad-Schafer MR, Schoffl H, Flaccus A, Lambert C, Biesalski HK. Inhibition of heme oxygenase-1 increases responsiveness of melanoma cells to ALA-based photodynamic therapy. Int J Oncol 2007; 31:1539-45.

[44] Parcellier A, Schmitt E, Brunet M, Hammann A, Solary E, Garrido C. Small heat shock proteins HSP27 and alphaB-crystallin: cytoprotective and oncogenic functions. Antioxid Redox Signal 2005; 7:404-13.

[45] Kocanova S, Buytaert E, Matroule JY*, et al.* Induction of heme-oxygenase 1 requires the p38MAPK and PI3K pathways and suppresses apoptotic cell death following hypericin-mediated photodynamic therapy. Apoptosis 2007; 12:731-41.

[46] Hanlon JG, Adams K, Rainbow AJ, Gupta RS, Singh G. Induction of Hsp60 by Photofrin-mediated photodynamic therapy. J Photochem Photobiol B 2001; 64:55-61.

[47] Verwanger T, Sanovic R, Aberger F, Frischauf AM, Krammer B. Gene expression pattern following photodynamic treatment of the carcinoma cell line A-431 analysed by cDNA arrays. Int J Oncol 2002; 21:1353-9.

[48] Jalili A, Makowski M, Switaj T*, et al.* Effective photoimmunotherapy of murine colon carcinoma induced by the combination of photodynamic therapy and dendritic cells. Clin Cancer Res 2004; 10:4498-508.

[49] Kuzelova K, Grebenova D, Pluskalova M, Marinov I, Hrkal Z. Early apoptotic features of K562 cell death induced by 5-aminolaevulinic acid-based photodynamic therapy. J Photochem Photobiol B 2004; 73:67-78.

[50] Yanase S, Nomura J, Matsumura Y*, et al.* Enhancement of the effect of 5-aminolevulinic acid-based photodynamic therapy by simultaneous hyperthermia. Int J Oncol 2005; 27:193-201.

[51] Prasmickaite L, Cekaite L, Hellum M, Hovig E, Hogset A, Berg K. Transcriptome changes in a colon adenocarcinoma cell line in response to photochemical treatment as used in photochemical internalisation (PCI). FEBS Lett 2006; 580:5739-46.

[52] Sugiyama M, Sakahara H, Sato K*, et al.* Evaluation of 3'-deoxy-3'-18F-fluorothymidine for monitoring tumor response to radiotherapy and photodynamic therapy in mice. J Nucl Med 2004; 45:1754-8.

[53] Romanko YS, Tsyb AF, Kaplan MA, Popuchiev VV. Relationship between antitumor efficiency of photodynamic therapy with photoditasine and photoenergy density. Bull Exp Biol Med 2005; 139:460-4.

[54] Togashi H, Uehara M, Ikeda H, Inokuchi T. Fractionated photodynamic therapy for a human oral squamous cell carcinoma xenograft. Oral Oncol 2006; 42:526-32.

[55] Park C, Lee I, Kang WK. Lovastatin-induced E2F-1 modulation and its effect on prostate cancer cell death. Carcinogenesis 2001; 22:1727-31.

[56] Finlan LE, Kernohan NM, Thomson G, Beattie PE, Hupp TR, Ibbotson SH. Differential effects of 5-aminolaevulinic acid photodynamic therapy and psoralen + ultraviolet A therapy on p53 phosphorylation in normal human skin in vivo. Br J Dermatol 2005; 153:1001-10.

[57] Crescenzi E, Varriale L, Iovino M, Chiaviello A, Veneziani BM, Palumbo G. Photodynamic therapy with indocyanine green complements and enhances low-dose cisplatin cytotoxicity in MCF-7 breast cancer cells. Mol Cancer Ther 2004; 3:537-44.

[58] Lu M, Xia L, Hua H, Jing Y. Acetyl-keto-beta-boswellic acid induces apoptosis through a death receptor 5-mediated pathway in prostate cancer cells. Cancer Res 2008; 68:1180-6.

[59] Bach LA. IGFBP-6 five years on; not so 'forgotten'? Growth Horm IGF Res 2005; 15:185-92.

[60] Koike H, Ito K, Takezawa Y, Oyama T, Yamanaka H, Suzuki K. Insulin-like growth factor binding protein-6 inhibits prostate cancer cell proliferation: implication for anticancer effect of diethylstilbestrol in hormone refractory prostate cancer. Br J Cancer 2005; 92:1538-44.

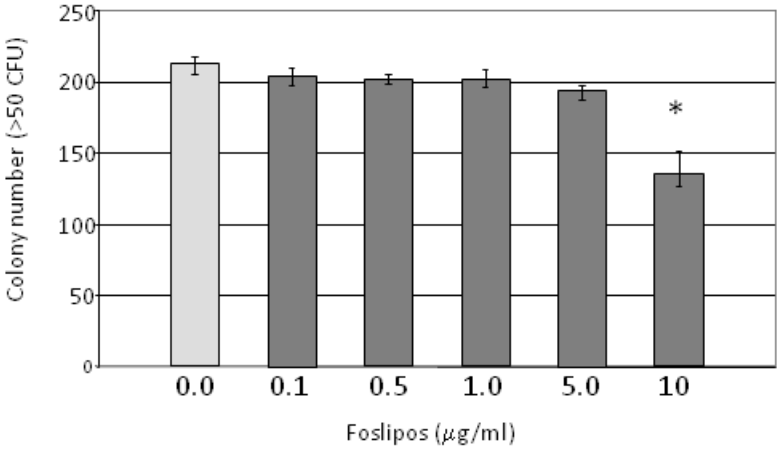
250
200
150
100
50
0
Colony number (>50 CFU)
*
0.0
0.1
0.5
1.0
5.0
10
Foslipos (μg/ml)

Fig 1

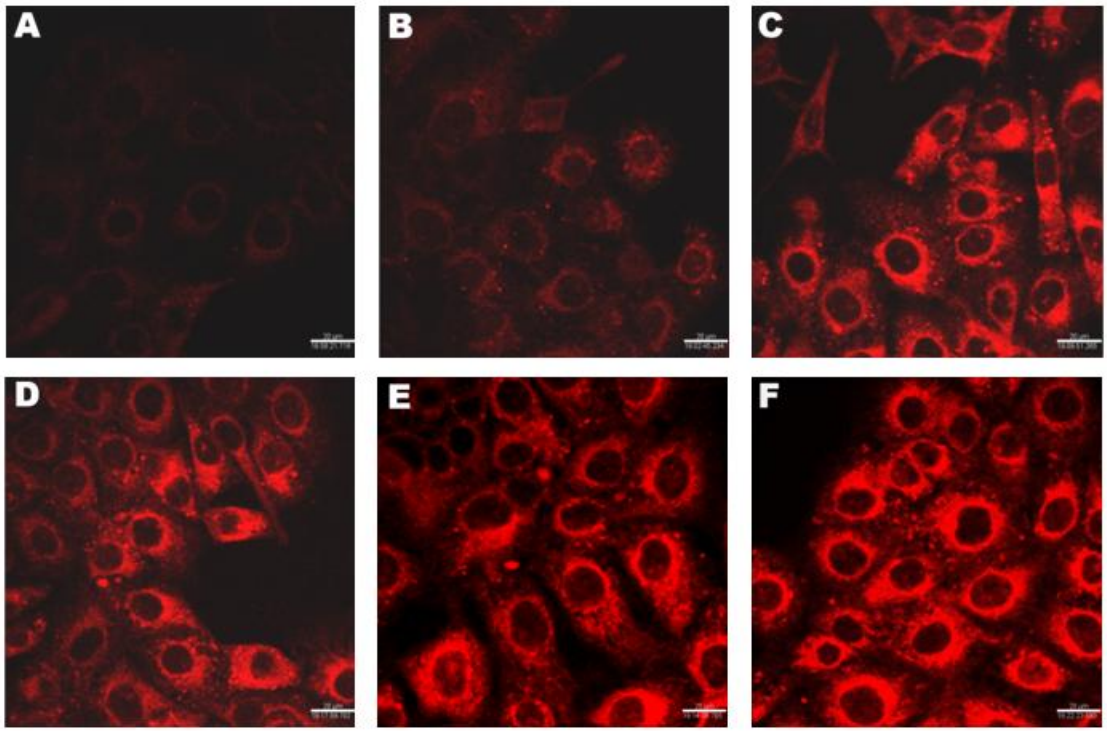

Fig. 2
Color reproduction only for the web

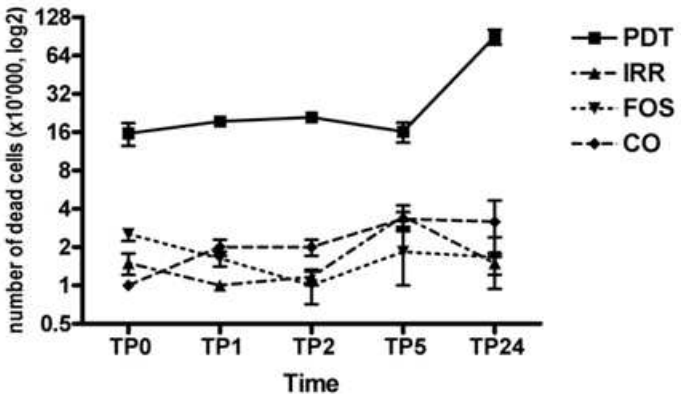
number of dead cells (x10'000, log2)
128
64
32
16
8
4
2
1
0.5
TP0
TP1
TP2
TP5
TP24
Time
PDT
IRR
FOS
CO

Fig. 3

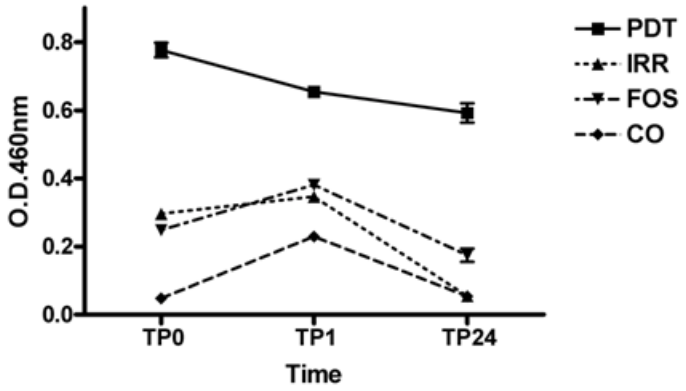

Fig. 4

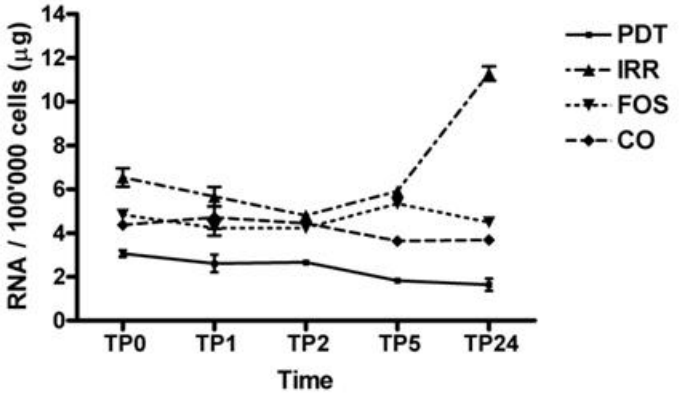
RNA / 100'000 cells (µg)
14
12
10
8
6
4
2
0
TP0
TP1
TP2
TP5
TP24
Time
PDT
IRR
FOS
CO

Fig. 5

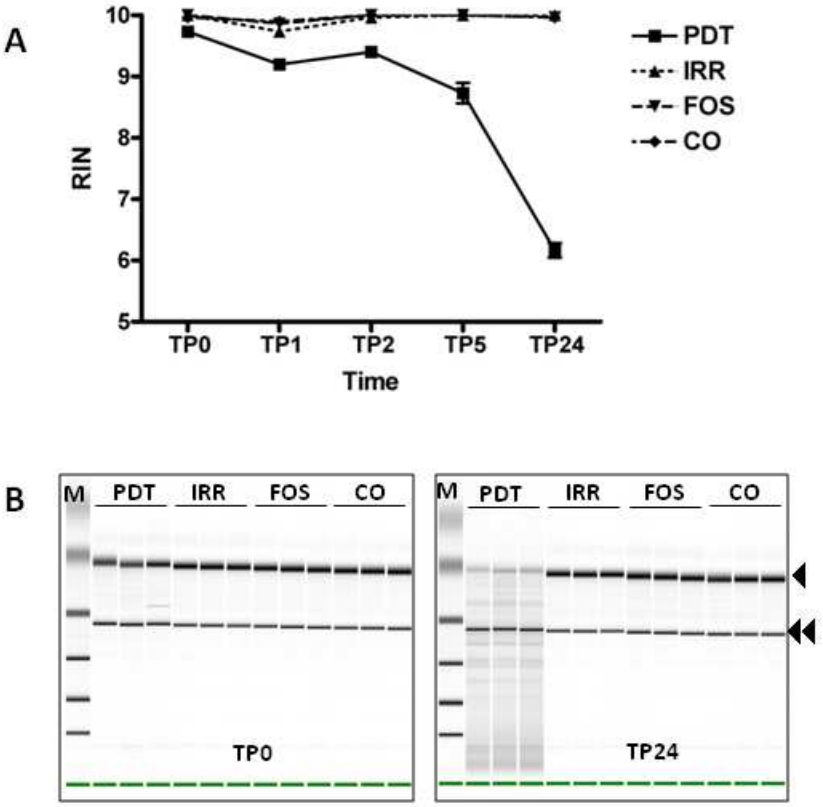
A
10
9
8
7
6
5
RIN
TP0
TP1
TP2
TP5
TP24
Time
PDT
IRR
FOS
CO
B
M
PDT
IRR
FOS
CO
TP0
M
PDT
IRR
FOS
CO
TP24

Fig. 6